Am J Otolaryngol 40 (2019) 547–554

Contents lists available at ScienceDirect

Am J Otolaryngol

journal homepage: www.elsevier.com/locate/amjoto

The molecular differences between human papillomavirus-positive and -negative oropharyngeal squamous cell carcinoma: A bioinformatics study

Jiaming Wang[a,1], Xiaoxi Xi[b,1], Wei Shang[c,1], Aneesha Acharya[d,e], Simin Li[f], Vuk Savkovic[g], Hanluo Li[g], Rainer Haak[f], Jana Schmidt[f], Xiangqiong Liu[h], Yupei Deng[h], Hongying Pan[i], Danilo Obradovic[j], Gerhard Schmalz[f,2], Dirk Ziebolz[f,3,*], Xianda Hu[k,3,*]

[a] The 16th Ward, Department of Ear, Nose and Throat (ENT), Daqing Oilfield General Hospital, Zhongkang Street No. 9, Saertu District, 163000, Daqing City, Heilongjiang Province, China
[b] Department of Stomatology, Northeast Petroleum University Affiliated Hospital, Fazhan Road, High Tech District, 163000 Daqing City, Heilongjiang Province, China
[c] Department of Stomatology, The Heping Affiliated Hospital of Changzhi Medical College, Changzhi City, Shanxi Province, China
[d] Faculty of Dentistry, University of Hong Kong, Hong Kong, China
[e] Dr D Y Patil Dental College and Hospital, Dr D Y Patil Vidyapeeth, Pimpri, Pune, India
[f] Department of Cariology, Endodontology and Periodontology, University Leipzig, Liebigstr. 12, 04103 Leipzig, Germany
[g] Saxon Incubator for Clinical Translation/Translational Centre for Regenerative Medicine, Leipzig University, Phillip-Rosenthal-Str. 55, Leipzig 04103, Germany
[h] Genomap Technologies, Kongjiang Road 1500, Yangpu District, Shanghai, China
[i] School of Dentistry, University of Michigan, USA
[j] Heart Center Leipzig, University of Leipzig, Strümpellstr. 39, 04289 Leipzig, Germany
[k] Laboratory of Molecular Cell Biology, Beijing Tibetan Hospital, China Tibetology Research Center, 218 Anwaixiaoguanbeili Street, Chaoyang, Beijing 100029, China

ARTICLE INFO

Keywords:
Human papillomavirus
Oropharyngeal squamous cell carcinoma
Genes
miRNAs
Pathways

ABSTRACT

Objective: To investigate the genetic and epigenetic differences between human papillomavirus (HPV)-positive oropharyngeal squamous cell carcinoma (OPSCC) and HPV-negative OPSCC.

Methods: Microarray data of HPV-positive and -negative OPSCC were retrieved from NCBI GEO datasets. Differentially expressed genes (DEGs) and differentially expressed miRNAs (DE-miRNAs) were identified by performing differential expression analysis. A functional enrichment analysis was performed to explore the biological processes and signaling pathways that DEGs and DE-miRNAs were involved in, respectively. A protein-protein interaction (PPI) network of DEGs was constructed to identify hub genes. miRNA-target network and miRNA-miRNA functional synergistic network were each constructed in order to identify risk-marker miRNAs. An miRNA-target-pathway network was constructed in order to explore the function of identified risk-marker miRNAs.

Results: Microarray data from 3 datasets (GSE39366, GSE40774, and GSE55550) was included and analyzed. The PPI network identified 3 hub genes (VCAM1, UBD, and RPA2). MiR-107 and miR-142-3p were found to play the most significant role in both the DE-miRNA-target network as well as in the miRNA-miRNA functional synergistic network. MiR-107 was involved in HPV-induced tumorigenesis by targeting many genes (CAV1, CDK6, MYB, and SERPINB5) and regulating the p53 signaling pathway, the PI3K-Akt signaling pathway, and the autophagy pathway. In addition, miR-142-3p was implicated in HPV-induced tumorigenesis by targeting the PPFIA1 gene and regulating transcriptional dysregulation and other cancerous pathways.

Conclusion: Three genes (VCAM1, UBD, and RPA2), two miRNAs (miR-107 and miR-142-3p), and four pathways (p53, PI3K-Akt, autophagy, and transcription dysregulation in cancer) were identified to play critical roles in distinguishing HPV-positive OPSCC from HPV-negative OPSCC.

* Corresponding authors.
E-mail addresses: Dirk.Ziebolz@medizin.uni-leipzig.de (D. Ziebolz), hellocean@hotmail.com (X. Hu).
[1] These authors contributed equally as the first author.
[2] Senior author: Dr. Gerhard Schmalz.
[3] These authors contributed equally as the corresponding authors.

https://doi.org/10.1016/j.amjoto.2019.04.015
Received 7 November 2018

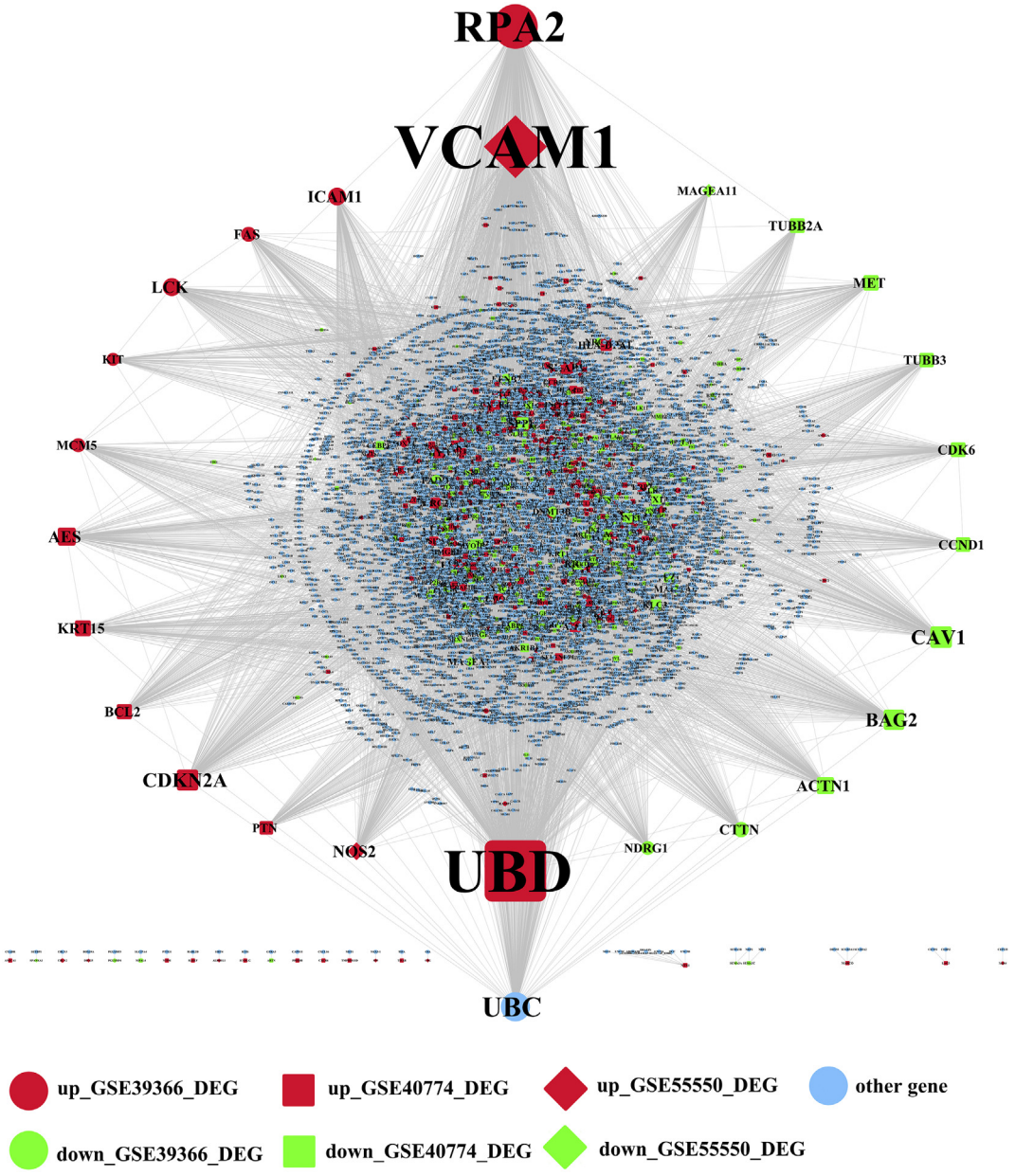

Fig. 1. The PPI network of DEGs.

1. Introduction

Head and neck squamous cell carcinoma (HNSCC), as the sixth most common cancer worldwide, remains a serious health problem due to its high incidence, late diagnosis, and low survival rate [1]. The human papillomavirus (HPV), in particular HPV16, has been established as a primary cause of the increasing incidence of HNSCC, mostly invading the oropharynx and causing oropharyngeal squamous cell carcinomas (OPSCC). Based on HPV status, OPSCC can be divided into two subtypes with different etiologies [2]. One subtype is induced by the persistent infection of HPV and is thus defined as HPV-positive (HPV+) OPSCC [2]. Another subtype of OPSCC is caused by alcohol and tobacco use, hence being defined as HPV-negative (HPV−) OPSCC [2]. Many systematic reviews [3–5] have summarized the discrepancy between these two subtypes of OPSCC tumors.

HPV-positive OPSCC differs from HPV-negative OPSCC in terms of clinical, radiological, histological, and prognostic characteristics. Regarding the clinical stage at presentation, HPV-positive tumors are more likely to be classified as early T stage (T1–T2) with higher N stage (usually cystic and multilevel), whereas metastases develop later in HPV-negative OPSCC [2]. Concerning radiological features, HPV(+) OPSCC tumors are more likely to demonstrate exophytic well-defined borders, whereas HPV(−) OPSCC tumors are likely to demonstrate invasion of adjacent structures [6]. From the histological perspective, HPV-positive OPSCCs are usually non-keratinizing, poorly differentiated, or basaloid squamous cell carcinomas; in contrast to this, HPV-negative OPSCCs are usually keratinizing [7]. Additionally, HPV (+) OPSCC patients have a more favorable prognosis and are more responsive to radio- and chemotherapy in comparison to HPV(−) OPSCC patients [4]. These clinical and biological differences any be attributable to the different molecular mechanisms underlying these 2 types of OPSCC tumors. Therefore, an understanding of tumor biology mechanisms in this regard would have implications for the development of tailored diagnostic and prognostic approaches.

In order to explore the molecular differences between HPV(+) OPSCCs and HPV(−) OPSCCs, several microarray studies [8–14] have

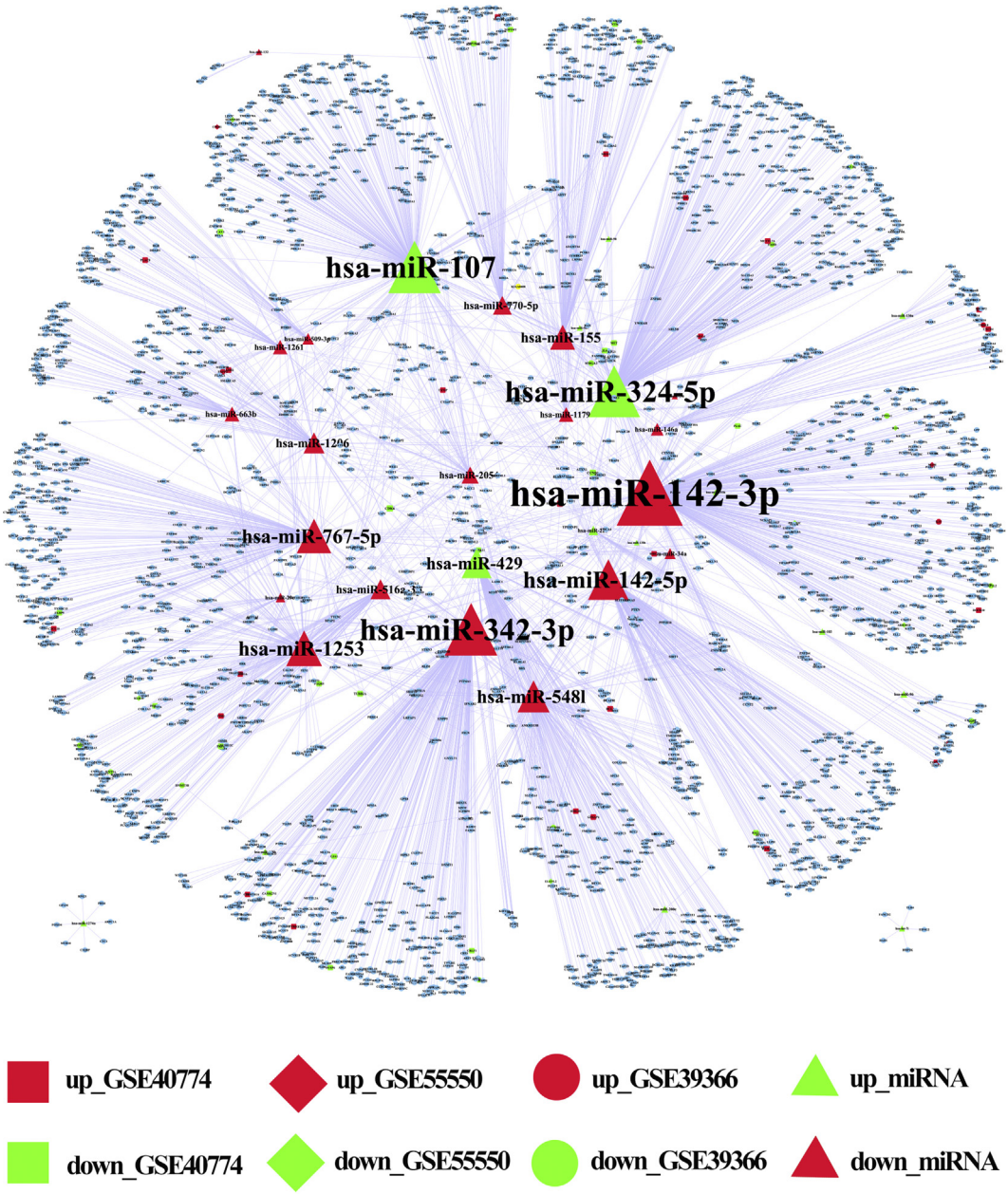

Fig. 2. The DEmiRNA-target genes regulatory network.

been conducted in recent years. One conducted microarray study [8] showed that genes involved in cell cycle regulation (CDKN2A), nuclear structure and meiosis (SYCP2), DNA replication and repair (RFC5), transcription regulation (ZNF238), cell differentiation (KLK8), and epidermis development (CRABP2) were expressed differently, when comparing HPV-positive OPSCCs to HPV-negative OPSCCs. Another microarray study [9] showed that DEGs expressed in HPV-positive OPSCC were mainly involved in cell cycle (CCNE2, E2F, CDC7 and CDKN2A) and cell proliferation (PCNA and Ki67), as well as DNA replication, recombination, and repair (XRCC1, DDB2, FANCG and TOPBP1). Although there are some overlapping results among these microarray studies, the variation among results are most likely attributable to different sample sizes, study designs, and different statistical approaches used by different microarray studies. Despite such heterogeneity, it is necessary to use bioinformatics techniques to integrate multiple microarray studies pertaining to this topic in order to comprehensively and systematically analyze the large body of data generated in these studies. To our knowledge, there is no existing reports that has applied bioinformatics techniques to investigate the genetic and epigenetic differences between HPV(+) OPSCC and HPV(−) OPSCC.

Thus, the aim of this bioinformatics study was to identify the potential genes, miRNAs, and significant signaling pathways that may underlie clinicopathological differences between HPV positive and HPV negative types of OPSCC. The molecular mechanisms thus identified could provide insight into the biological effects of HPV infection in OPSCC pathogenesis, and could be developed as novel therapeutic targets in OPSCC treatment.

2. Material and methods

2.1. Procurement of data

Datasets related to OPSCC were researched using the GEO database (https://www.ncbi.nlm.nih.gov/gds/) and genetic data including both HPV(+) OPSCC and HPV(−) OPSCC tissue samples was downloaded. In accordance with the definition of OPSCC, the included sampling sites

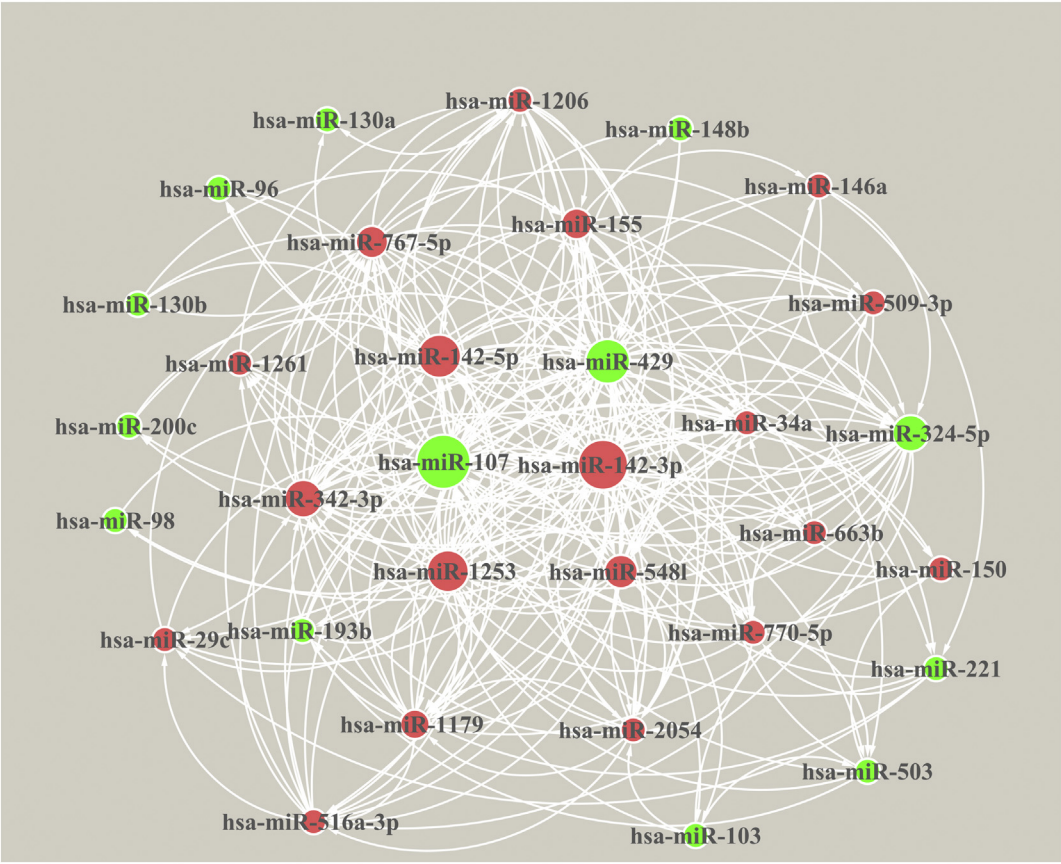

Fig. 3. The miRNA-miRNA synergistic functional network. The red nodes represent up-regulated miRNAs, whereas the green nodes represent down-regulated miRNAs. (For interpretation of the references to color in this figure legend, the reader is referred to the web version of this article.)

were restricted to the oropharynx, consisting of the soft palate, base (or posterior one-third) of tongue, palatine tonsils, palatoglossal folds, valleculae, and posterior pharyngeal wall [15]. The experimental group included HPV(+) OPSCC samples, whereas the control group included HPV(−) OPSCC samples. Based on this inclusion criteria, 6 mRNA expression profiling datasets (GSE56142, GSE72536, GSE65858, GSE39366, GSE55550, and GSE40774) and one miRNA expression profiling dataset (GSE82064) were downloaded (Table S1).

In order to avoid the errors caused by the heterogeneity in terms of sample size, the datasets containing > 10 samples in both the experimental group and the control group were selected. Consequently, two datasets (GSE56142 and GSE72536) with a small sample size were excluded as the sample size of the control group was 2 for GSE56142 dataset and 4 for GSE72536 dataset. The number of DEGs in the GSE65858 dataset was too small, thus leading to the exclusion of this dataset to avoid errors based on insufficient material. The three mRNA expression profiling datasets (GSE39366, GSE55550, and GSE40774) were finally included in the study.

2.2. Differential expression analysis

Regarding the miRNA and mRNA expression profiling data, differential expression analysis was performed by using the "*limma*" package. For gene sequencing data, differential expression analysis was performed using the *edgeR* package. If a gene or miRNA had a p value of < 0.05 and $|\log FC| > 1$, this gene or miRNA was defined as differentially expressed. The genes or miRNAs with $\log FC > 1$ were considered to be up-regulated, whereas the genes or miRNAs with $\log FC < -1$ were regarded as down-regulated.

2.3. Functional enrichment analysis

Functional enrichment analysis of differentially expressed genes (DEGs) was performed by using the Functional Enrichment analysis tool (Funrich, version 3.1.3, http://www.funrich.org/). The significant level (p value) of each pathway was calculated based on hypergeometric distribution. The results of multiple hypothesis tests were corrected and a false positive rate (FDR) was obtained. The pathways with p values of < 0.05 were considered as significant.

2.4. Constructing PPI network of DEGs

Experimentally validated PPI interaction pairs were obtained from many databases including HPRD (http://www.hprd.org/), STRING (https://string-db.org/newstring_cgi/show_input_page.pl?UserId=RxNdJERjemqw&sessionId=5C0iOmbkcoyH), IntAct (http://www.ebi.ac.uk/intact/), MINT(http://mint.bio.uniroma2.it/mint/Welcome.do), BioGrid (http://thebiogrid.org/), and DIP (http://dip.doe-mbi.ucla.edu/dip/Main.cgi). A total of 280,826 PPI pairs corresponding to 19,610 genes were obtained. Using the obtained PPI interaction pairs corresponding to the DEGs, a PPI network was constructed and visualized with Cytoscape software and topological characteristics of the PPI network were analyzed.

2.5. Construction of miRNA-gene regulatory network

In order to further investigate the functions of DE-miRNAs, an miRNA-gene regulatory network was constructed. Experimentally validated miRNA-target interaction pairs were downloaded from different databases including miR2Disease (http://www.mir2disease.org/), miRecords (http://miRecords.umn.edu/miRecords), and miRTarbase

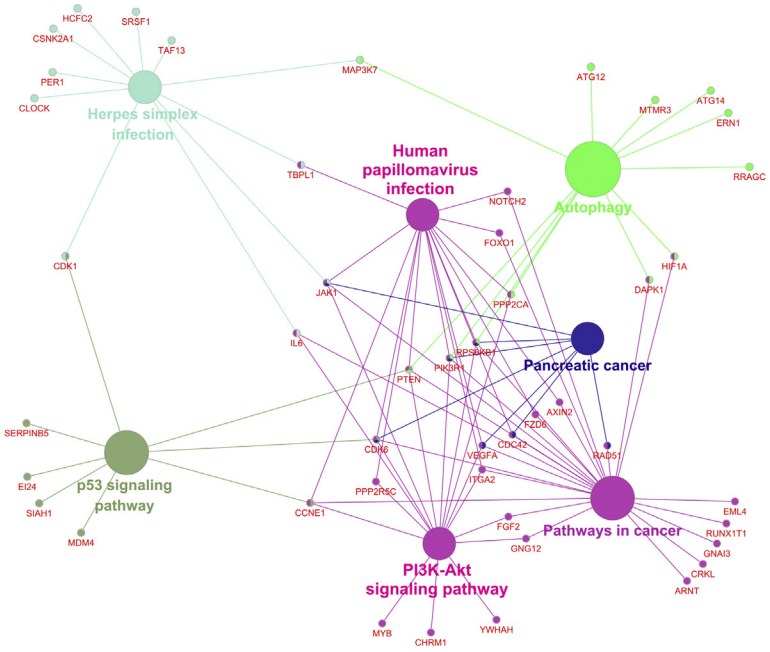

a. hsa-miR-107

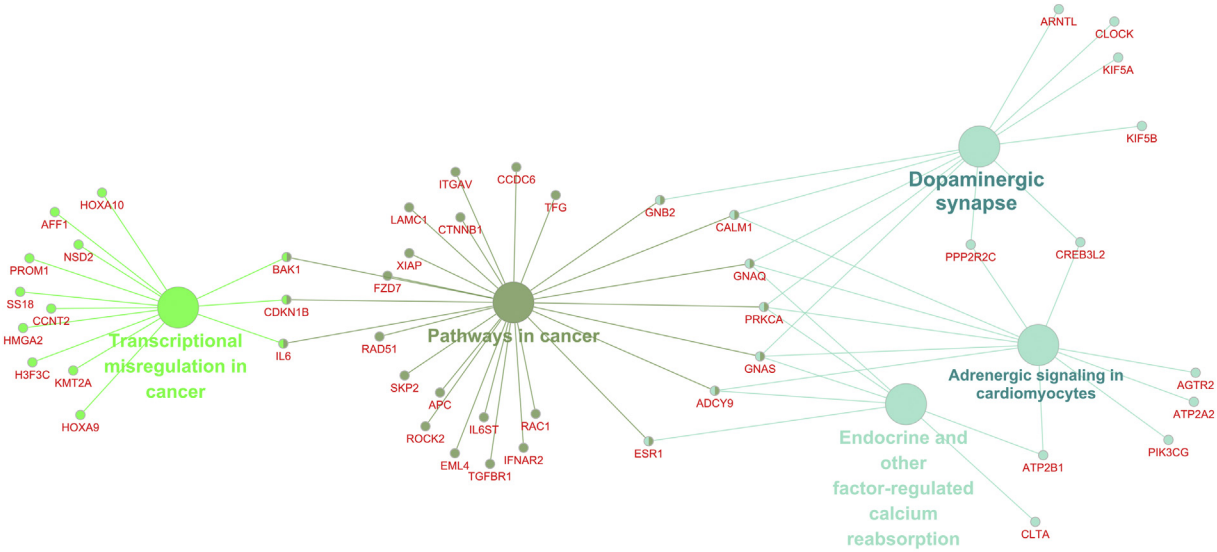

b. hsa-miR-142-3p

Fig. 4. The miRNA-target-pathway network of two significant miRNAs (miR-107 and miR-142-3p).

(http://miRTarBase.mbc.nctu.edu.tw). Finally, a total of 383,472 miRNA-target interaction pairs were obtained, consisting of 2827 miRNAs and 15,474 target genes. miRNA-target interaction pairs corresponding to DE-miRNAs were used to construct an miRNA-target regulatory network, which was visualized in Cytoscape software. The topological characteristics of this network were calculated and the top 10 miRNAs were determined.

2.6. Construction of miRNA-miRNA functional synergistic network (MFSN)

In order to analyze the interactive functions between different miRNAs, pairs of DE-miRNAs were obtained and used to identify related mRNAs commonly targeted by both DE-miRNAs. The functions of these commonly related DE-miRNAs were used to determine enriched 'biological processes' (BP) in the Gene Ontology (GO) terminology. Each enriched BP was considered as a functional module. If the miRNA-miRNA interaction pairs had at least one functional module, they were considered to possess a synergistic role. The miRNA-miRNA interaction pairs with synergistic roles were determined and used to construct a genome scale miRNA-miRNA functional synergistic network (MFSN).

2.7. Validation of risk-marker miRNAs and their target genes

The effects of risk-marker miRNAs in the GSE82064 dataset was evaluated using a support vector machine (SVM) approach, which is a machine learning technique. Subsequently, mRNA data of six datasets

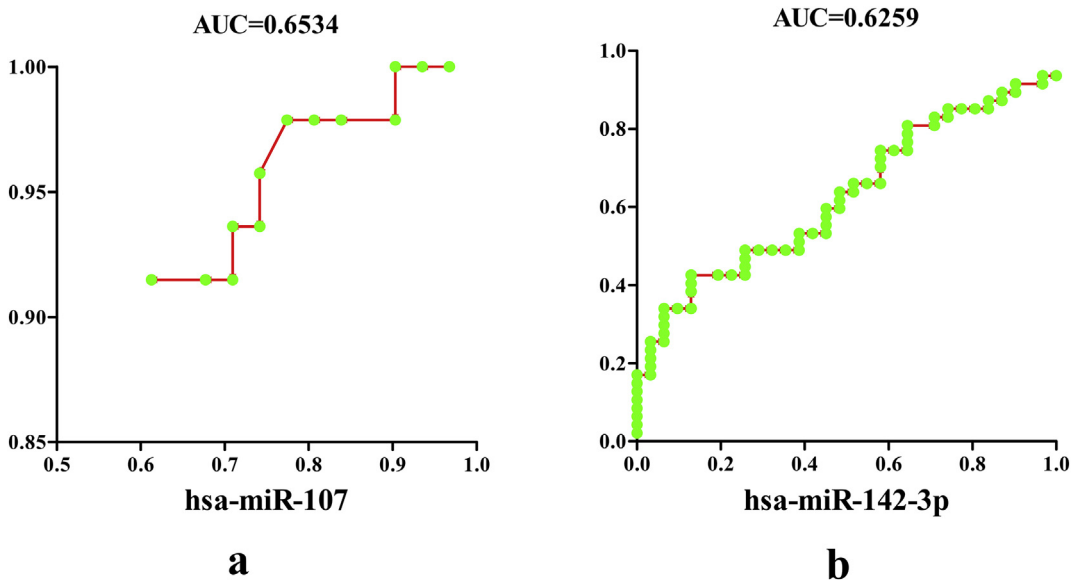

Fig. 5. The ROC curves of two miRNAs (miR-107 and miR-142-3p).

(GSE56142, GSE65858, GSE39366, GSE55550, GSE72536, and GSE40774) was used to validate the accuracy of predicted results. Receiver operating characteristic curves (ROC) of the identified risk-marker miRNAs were drawn and area under curve (AUC) values were calculated. Additionally, functions of the top 5 genes targeted by the identified risk-marker miRNAs were also determined.

3. Results

3.1. Identification of DEGs

Differential expression analyses were using data sourced from 6 databases including GSE39366, GSE55550, GSE40774, GSE72536, GSE56142, and GSE65858. DEGs expressed between HPV positive samples and HPV negative samples were determined. The numbers of identified up-regulated and down-regulated DE-mRNAs are shown in Table S2. Among these DEGs, 18 down-regulated DEGs (Fig. S1a) and 7 up-regulated DEGs (Fig. S1b) overlapped between 3 datasets. Since only a small number of DEGs were found to overlap in 3 datasets, all DEGs were analyzed further.

3.2. Functional enrichment analysis

Biological processes and signaling pathways that the identified DEGs were involved in were determined using a hypergeometric test. Fig. S2a shows that the DEGs were mainly involved in biological processes of immune response, cell growth and/or maintenance, cell communication, and signal transduction. A total of 135 significant signaling pathways were determined, and the top 15 pathways were extracted, as shown in Fig. S2b. The most significant pathways that DEGs were involved in are the ErbB receptor signaling network, VEGF and VEGFR signaling network, and the Internalization of ErbB1 (Fig. S2b).

3.3. Construction of PPI network

The PPI network (Fig. 1) consisted of a total of 6696 nodes and 15,482 edges. The topological characteristics of the network were calculated and are presented in Table S3. It was evident that the gene with the highest degree in this PPI network was VCAM1.

3.4. Differential expression analysis of miRNAs

A total of 41 differentially expressed miRNAs (DE-miRNAs) were identified, including 17 down-regulated DE-miRNAs and 24 up-regulated DE-miRNAs. A total of 3151 miRNA-target interaction pairs were identified, including 35 DE-miRNAs and 2519 target genes. Fig. S3a shows that DE-miRNAs were mainly involved in biological processes such as the regulation of nucleobase, nucleoside, as well as nucleotide and nucleic acid metabolism. In addition, Fig. S3b shows that DE-miRNAs were mainly involved in several pathways including the TRAIL signaling pathway, the mTOR signaling pathway, and the PDGFR-beta signaling pathway.

3.5. Construction of miRNA-target network and MFSN network

By using identified miRNA-target interaction pairs, the miRNA-target genes regulatory network (Fig. 2) was constructed, including 3151 interaction pairs and 2561 nodes. Based on the miRNA targets, a total of 264 miRNA-miRNA interaction pairs were obtained, using 32 miRNAs. With these interaction pairs, the MFSN network was constructed, as shown in Fig. 3. The topological characteristics of this network were analyzed and are depicted in Table S5. It was shown that miR-107 and miR-142-3p regulated the highest number of miRNAs.

Validation of risk-marker miRNAs and their target genes miR-107 and miR-142-3p played the most important role in regulating the miRNA-target network and the MFSN network (Table S5). MiR-107 was down-regulated in HPV positive samples, while miR-142-3p was up-regulated in HPV negative samples. The miRNA-target-pathway network was depicted in Fig. 4. The effects miR-107 and miR-142-3p in the GSE82064 dataset and their related ROC curves are depicted in Fig. 5. The ROC values are presented in Table S6 which showed the classified effects of CAV1 and CDK6 were comparatively balanced among the 6 datasets. The prediction accuracy of CAV1 and CDK6 was comparatively higher than other genes (MYB, SERPINB5, and PPFIA1). Both CAV1 and CDK6 were targeted by miR-107, and had a higher degree than the other 3 determined target genes (MYB, SERPINB5, and PPFIA1).

4. Discussion

Several molecular differences emerged between HPV positive and negatives types of OPSCC. These may be critical to understanding the

cause of differences in clinical presentation and develop more tailored regimes for successful management. The top 10 proteins (VCAM1, UBD, RPA2, UBC, CAV1, CDKN2A, BAG2, AES, NOS2, LCK) identified in the PPI network seem to play a critical role in causing the distinct clinical and pathological features of HPV+ and HPV− OPSCC. These findings are largely congruent with existing experimental evidence. The top 3 proteins with the highest degree were (VCAM1, UBD, RPA2) whereas CDKN2A has been most well studied in previous investigations [16–18]. Vascular Cell Adhesion Molecule 1 (VCAM1), with the highest degree in PPI network, is involved in B cell activation, and this tumor-infiltrating B-cells associated signal is suggested to segregate HPV(+) from HPV (−) tumors [13]. UBD (ubiquitin D) can promote TNF-alpha-mediated proteasomal degradation of ubiquitinated-I-kappa-B-alpha, thus further regulating the activation of the central mediator of innate immunity NF-kappa-B [13]. These findings suggest that HPV related oncoproteins may modulate the TNF signaling pathway and possibly regulate the activation of the NF-κB pathway, possibly by dysregulation of UBD [19]. RPA2, the 32-kDa subunit of Replication protein A (RPA), was previously shown as upregulated in HPV positive OPSCC [9]. RPA is the major human single-stranded DNA (ssDNA)-binding protein complex and plays a role in many facets of DNA metabolism such as DNA replication, repair, and recombination [20]. The HPV protein E1, an ATP-dependent viral DNA helicase, can recruit RPA to the viral origin of replication and physically interact with RPA during papillomavirus DNA replication [20]. The cyclin-dependent kinase inhibitor 2A (CDKN2A, also called p16) is shown to be differentially overexpressed in HPV-infected OPSCC, by multiple studies [3,8,12], and is involved in DNA replication and cell cycle regulation. Expression of p16 is increased in HPV infections by HPV E7 oncoprotein inactivation of the pRB tumor suppressor, resulting in a loss of p16 suppression [21].

Among the 32 identified risk-marker miRNAs, 2 miRNAs (miR-107 and miR-142-3p) had the highest degree in the miRNA-miRNA synergistic functional network, and played the most important roles in segregating HPV positive from HPV negative OPSCC. The signaling pathways regulated by these 2 significant miRNAs emergent in the study and their known roles in HPV associated OPSCC will be described as follows. In a previous study, MiR-107 was downregulated in HPV positive OPSCC and significantly associated with overall survival and disease free survival of this type of malignancy [22]. MiR-107 appears to be involved in HPV-induced tumorigenesis by regulating multiple signaling pathways, including the p53 signaling pathway, PI3K-Akt signaling pathway, autophagy, and herpes simplex infections. For instance, the HPV oncoprotein E6 can induce degradation of p53 by directly binding to the ubiquitin ligase E6AP, inhibiting p53-dependent signaling upon stress stimuli, and contributing to tumorigenesis [23]. In addition to the inhibition of the p53 signaling pathway, HPV infections accompanied by E6/E7 expression can activate the PI3K/Akt/mTOR signaling pathway, which can contribute to the immortalization and carcinogenesis of HPV-transduced cells and thus modulate tumor initiation and progression [24]. Furthermore, the expression of the oncoviral proteins E5, E6, and E7 can drive the inhibition and impairment of an autophagic response by acting at the initial and at the late step of the viral infection and carcinogenesis [25]. Additionally, genes targeted by miR-107, included CAV1, CDK6, MYB, and SERPINB5. The upregulation of Caveolin-1 (CAV1) plays a critical role in negatively regulating cell cycle progression by arresting cells in the G(0)/G(1) phase of the cell cycle [26]. In addition, the HPV E6 viral oncoprotein can down-regulate CAV1 by inactivating tumor suppressor p53 [27]. CDK6 (cyclin-dependent kinase 6) is downregulated by tumor suppressor p16, which is a cyclin-dependent kinase inhibitor. Since the p16 protein has been increasingly recognized as a reliable surrogate marker for survival in HR (high risk) HPV positive OPSCC, CDK6 could be also believed to be related to the prognosis of HPV(+) OPSCC. MYB (also known as c-myb) upregulation can transactivate the HPV-16 promoter/enhancer, which occurs with HPV-associated cell transformation. Thus, this transcription factor seems to be involved carcinogenesis of HPV positive OPSCC [28]. SERPINB5 (Serpin peptidase inhibitor, clade B (ovalbumin), member 5) has been found as overexpressed in women with a persistent HPV16 infection when compared to HPV-negative women [29]. Taken together with existing evidence, there seems to be significant regulatory role of miR-107 in distinguishing HPV(+) OPSCC from HPV(−) OPSCC.

In addition, miR-142-3p has also previously been identified to play critical roles in HPV-induced carcinogenesis. MiR-142-3p has been implicated in many inflammatory diseases and cancers, being noted as dysregulated in LPS-induced immune responses in periodontal diseases [30] and up-regulated in HPV-driven OPSCC [31], therefore suggested to be a prognostic marker of head and neck cancer [32]. This miRNA can target the PPFIA1 gene (PTPRF interacting protein alpha 1; also known as LIP1, or LIPRIN) and is also involved in many signaling pathways such as transcriptional dysregulation in cancer, dopaminergic synapse, and endocrine and other factor-regulated calcium reabsorption processes. Its target PPFIA1 gene has been found to be downregulated in HPV RNA-positive tumors. The protein encoded by PPFIA1 regulates the disassembly of focal adhesion [33], which determines the rate of cell migration during the processes of cancer cell invasion and metastasis [34]. The human papillomavirus E6 oncogene has the ability to repress the cell adhesion pathway and thus further disrupt focal adhesion [35]. Based on this evidence, the downregulation of PPFIA1 may be involved in tumorigenesis of HPV-driven OPSCC by disrupting the disassembly of focal adhesion. In addition, the “transcriptional dysregulation in cancer” signaling pathway targeted by miR-107 has been reported as one of the main enriched pathways of breakpoints from RNA samples of HPV as HPV integration sites were enriched in transcription factor binding sites (TFBS) [36]. HPV integration may directly trigger the abnormal transcription and interrupt DNA repair mechanisms, thus inducing tumorigenesis in OPSCC. The other identified pathways (e.g., dopaminergic synapse, endocrine and other factor-regulated calcium reabsorption) targeted by miR-107 are not supported to be related to the HPV-driven OPSCC tumorigenesis by existing experimental studies, thus their putative roles should be researched further.

Both strengths and limitations of this study should be considered while interpreting the outcomes. Firstly, all public datasets examining HPV-positive and HPV-negative OPSC samples were included, except for two datasets with very small sample sizes. Integrating data from a large number of samples is the key advantage of secondary bioinformatics analysis, which lends itself to more statistical robustness. Secondly, various types of molecular entities (genes, miRNAs, biological processes, and signaling pathways) were identified by performing a series of comprehensive analytical methods, including functional enrichment analysis, PPI network analysis, miRNA-target network analysis, miRNA-miRNA synergistic functional network analysis, and miRNA-target-pathway network analysis. Despite these advantages, this study also has some notable limitations. Only 1 miRNA expression profiling dataset was identified and included. More primary studies applying open-ended methods should investigate the alteration of miRNA expression profiles between HPV(+) and HPV(−) OPSCCs. A second limitation is that we did not investigate the molecular differences between the HPV-active (DNA+RNA+) type and the HPV-inactive (DNA+RNA−) type of OPSCCs, both of which belong to the HPV-positive type as only 1 dataset (GSE55550) included in this study distinguished between HPV-active and HPV-inactive OPSCCs. The results of this microarray dataset (GSE55550) showed that HPV-inactive OPSCC has gene expression profiles that are distinguishable from those of both HPV-active and HPV-negative OPSCC, suggesting that these may constitute an individual pathogenetic group [12]. This finding has implications for the experimental design of future microarray studies whereby OPSCC samples of 3 types HPV-active, inactive, and negative types should be characterized. Another limitation of the current study is that only bioinformatics techniques were applied, and a verification of the results through PCR experiments was not performed due to limited

funding. However, the bioinformatics identification of these putative molecular entities may serve as the basis for future laboratorial studies and research.

In summary, based on the results of this exploratory study the several hypotheses may be formed. First, we hypothesize that HPV infection engages ErbB signaling in OPSCC oncogenesis by altering cellular growth. A second hypothesis is that VEGF signaling machinery is exploited in HPV mediated OPSCC for tumor angiogenesis. Thirdly, we propose that VCAM1 overexpression facilitated by HPV infection may be involved in OPSCC immune subversion. Furthermore, HPV oncoproteins may mediate hijacking of ubiquitination processes and interfere with DNA repair, marked by UBD and RPA2, respectively. We also suggest MiR-107 and miR-142-3p expression levels together may be used as risk-markers of HPV positive OPSCC. Lastly, we hypothesize that p53, PI3K-Akt, autophagy, and transcription dysregulation pathways are the key differentiators of HPV associated OPSCC oncogenesis mechanisms versus non-HPV associated oncogenesis.

5. Conclusion

Three genes (VCAM1, UBD, and RPA2), 2 miRNAs (MiR-107 and miR-142-3p), and multiple pathways (p53, PI3K-Akt, autophagy, and transcription dysregulation in cancer) were identified to play critical roles in distinguishing HPV-positive OPSCC from HPV-negative OPSCC. These specific molecular mechanisms may comprise valuable targets for OPSCC research in future experimental studies.

Supplementary data to this article can be found online at https://doi.org/10.1016/j.amjoto.2019.04.015.

Conflicts of interests

The authors declare no potential conflict of interests with respect to the authorship and/or publication of this paper.

Acknowledgements

Simin Li (CSC No: 201608080010) and Hanluo Li (CSC No: 201308080064) were supported by the China Scholarship Council (CSC) for doctor study at University Leipzig.

References

[1] Sanderson RJ, Ironside JA. Squamous cell carcinomas of the head and neck. BMJ (Clin Res Ed) 2002;325(7368):822–7.
[2] Elrefaey S, Massaro MA, Chiocca S, Chiesa F, Ansarin M. HPV in oropharyngeal cancer: the basics to know in clinical practice. Acta Otorhinolaryngol Ital 2014;34(5):299–309.
[3] van Kempen PM, Noorlag R, Braunius WW, Stegeman I, Willems SM, Grolman W. Differences in methylation profiles between HPV-positive and HPV-negative oropharynx squamous cell carcinoma: a systematic review. Epigenetics 2014;9(2):194–203.
[4] Selcuk OT. Human papillomavirus positive oropharyngeal cancer: the general information. Egypt J Ear Nose Throat Allied Sci 2016;17(3):127–32.
[5] Wang MB, Liu IY, Gornbein JA, Nguyen CT. HPV-positive oropharyngeal carcinoma: a systematic review of treatment and prognosis. Otolaryngol Head Neck Surg 2015;153(5):758–69.
[6] Cantrell SC, Peck BW, Li G, Wei Q, Sturgis EM, Ginsberg LE. Differences in imaging characteristics of HPV-positive and HPV-negative oropharyngeal cancers: a blinded matched-pair analysis. AJNR Am J Neuroradiol 2013;34(10):2005–9.
[7] Fakhry C, Lacchetti C, Rooper LM, Jordan RC, Rischin D, Sturgis EM, et al. Human papillomavirus testing in head and neck carcinomas: ASCO clinical practice guideline endorsement of the College of American Pathologists Guideline. J Clin Oncol 2018;36(31):3152–61. [Jco1800684].
[8] Martinez I, Wang J, Hobson KF, Ferris RL, Khan SA. Identification of differentially expressed genes in HPV-positive and HPV-negative oropharyngeal squamous cell carcinomas. Eur J Cancer 2007;43(2):415–32.
[9] Lohavanichbutr P, Houck J, Fan W, Yueh B, Mendez E, Futran N, et al. Genomewide gene expression profiles of HPV-positive and HPV-negative oropharyngeal cancer: potential implications for treatment choices. Arch Otolaryngol Head Neck Surg 2009;135(2):180–8.
[10] Wichmann G, Rosolowski M, Krohn K, Kreuz M, Boehm A, Reiche A, et al. The role of HPV RNA transcription, immune response-related gene expression and disruptive TP53 mutations in diagnostic and prognostic profiling of head and neck cancer. Int J Cancer 2015;137(12):2846–57.
[11] Walter V, Yin X, Wilkerson MD, Cabanski CR, Zhao N, Du Y, et al. Molecular subtypes in head and neck cancer exhibit distinct patterns of chromosomal gain and loss of canonical cancer genes. PloS One 2013;8(2):e56823.
[12] Tomar S, Graves CA, Altomare D, Kowli S, Kassler S, Sutkowski N, et al. Human papillomavirus status and gene expression profiles of oropharyngeal and oral cancers from European American and African American patients. Head Neck 2016;38(Suppl. 1):E694–704.
[13] Wood O, Woo J, Seumois G, Savelyeva N, McCann KJ, Singh D, et al. Gene expression analysis of TIL rich HPV-driven head and neck tumors reveals a distinct B-cell signature when compared to HPV independent tumors. Oncotarget 2016;7(35):56781–97.
[14] Keck MK, Zuo Z, Khattri A, Stricker TP, Brown CD, Imanguli M, et al. Integrative analysis of head and neck cancer identifies two biologically distinct HPV and three non-HPV subtypes. Clin Cancer Res 2015;21(4):870–81.
[15] Chi AC, Day TA, Neville BW. Oral cavity and oropharyngeal squamous cell carcinoma—an update. CA Cancer J Clin 2015;65(5):401–21.
[16] Chernock RD, Wang X, Gao G, Lewis Jr. JS, Zhang Q, Thorstad WL, et al. Detection and significance of human papillomavirus, CDKN2A(p16) and CDKN1A(p21) expression in squamous cell carcinoma of the larynx. Mod Pathol 2013;26(2):223–31.
[17] Gronhoj Larsen C, Gyldenlove M, Jensen DH, Therkildsen MH, Kiss K, Norrild B, et al. Correlation between human papillomavirus and p16 overexpression in oropharyngeal tumours: a systematic review. Br J Cancer 2014;110(6):1587–94.
[18] Chen WS, Bindra R, Mo A, Hayman T, Husain Z, Contessa JN, et al. CDKN2A Copy Number Loss in HPV− and HPV+ Head and Neck Cancer to Indicate Poor Prognosis: An Integrated Genomic and Clinical TCGA Analysis. vol. 35. 2017. [15_suppl):6060-].
[19] James MA, Lee JH, Klingelhutz AJ. Human papillomavirus type 16 E6 activates NF-kappaB, induces cIAP-2 expression, and protects against apoptosis in a PDZ binding motif-dependent manner. J Virol 2006;80(11):5301–7.
[20] Loo YM, Melendy T. Recruitment of replication protein A by the papillomavirus E1 protein and modulation by single-stranded DNA. J Virol 2004;78(4):1605–15.
[21] Liu SZ, Zandberg DP, Schumaker LM, Papadimitriou JC, Cullen KJ. Correlation of p16 expression and HPV type with survival in oropharyngeal squamous cell cancer. Oral Oncol 2015;51(9):862–9.
[22] Hui AB, Lin A, Xu W, Waldron L, Perez-Ordonez B, Weinreb I, et al. Potentially prognostic miRNAs in HPV-associated oropharyngeal carcinoma. Clin Cancer Res 2013;19(8):2154–62.
[23] Buitrago-Perez A, Garaulet G, Vazquez-Carballo A, Paramio JM, Garcia-Escudero R. Molecular signature of HPV-induced carcinogenesis: pRb, p53 and gene expression profiling. Curr Genomics 2009;10(1):26–34.
[24] Zhang L, Wu J, Ling MT, Zhao L, Zhao KN. The role of the PI3K/Akt/mTOR signalling pathway in human cancers induced by infection with human papillomaviruses. Mol Cancer 2015;14:87.
[25] Mattoscio D, Medda A, Chiocca S. Human papilloma virus and autophagy. Int J Mol Sci 2018;19(6).
[26] Galbiati F, Volonte D, Liu J, Capozza F, Frank PG, Zhu L, et al. Caveolin-1 expression negatively regulates cell cycle progression by inducing G(0)/G(1) arrest via a p53/p21(WAF1/Cip1)-dependent mechanism. Mol Biol Cell 2001;12(8):2229–44.
[27] Razani B, Altschuler Y, Zhu L, Pestell RG, Mostov KE, Lisanti MP. Caveolin-1 expression is down-regulated in cells transformed by the human papilloma virus in a p53-dependent manner. Replacement of caveolin-1 expression suppresses HPV-mediated cell transformation. Biochemistry 2000;39(45):13916–24.
[28] Nurnberg W, Artuc M, Nawrath M, Lovric J, Stuting S, Moelling K, et al. Human c-myb is expressed in cervical carcinomas and transactivates the HPV-16 promoter. Cancer Res 1995;55(19):4432–7.
[29] Manawapat-Klopfer A, Thomsen LT, Martus P, Munk C, Russ R, Gmuender H, et al. TMEM45A, SERPINB5 and p16INK4A transcript levels are predictive for development of high-grade cervical lesions. Am J Cancer Res 2016;6(7):1524–36.
[30] Schmalz G, Li S, Burkhardt R, Rinke S, Krause F, Haak R, et al. MicroRNAs as salivary markers for periodontal diseases: a new diagnostic approach? Biomed Res Int 2016;2016:1027525.
[31] Gao G, Gay HA, Chernock RD, Zhang TR, Luo J, Thorstad WL, et al. A microRNA expression signature for the prognosis of oropharyngeal squamous cell carcinoma. Cancer 2013;119(1):72–80.
[32] Summerer I, Unger K, Braselmann H, Schuettrumpf L, Maihoefer C, Baumeister P, et al. Circulating microRNAs as prognostic therapy biomarkers in head and neck cancer patients. Br J Cancer 2015;113(1):76–82.
[33] Serra-Pages C, Kedersha NL, Fazikas L, Medley Q, Debant A, Streuli M. The LAR transmembrane protein tyrosine phosphatase and a coiled-coil LAR-interacting protein co-localize at focal adhesions. EMBO J 1995;14(12):2827–38.
[34] Turnover of focal adhesions and cancer cell migration. Int J Cell Biol 2012;2012.
[35] Ben Khalifa Y, Teissier S, Tan MK, Phan QT, Daynac M, Wong WQ, et al. The human papillomavirus E6 oncogene represses a cell adhesion pathway and disrupts focal adhesion through degradation of TAp63beta upon transformation. PLoS Pathog 2011;7(9):e1002256.
[36] Li W, Qi Y, Cui X, Huo Q, Zhu L, Zhang A, et al. Characteristic of HPV integration in the genome and transcriptome of cervical cancer tissues. J BioMed Res Int 2018;2018:7.